

Probing minimal supergravity in the type-I seesaw mechanism with lepton flavor violation at the CERN LHC

M. Hirsch* and J. W. F. Valle⁺

AHEP Group, Instituto de Física Corpuscular – C.S.I.C./Universitat de València Edificio de Institutos de Paterna, Apartado 22085, E-46071 València, Spain

W. Porod[‡]

Institut für Theoretische Physik und Astronomie, Universität Würzburg Am Hubland, 97074 Wuerzburg

J. C. Romao[§] and A. Villanova del Moral^{||}

Departamento de Física and CFTP, Instituto Superior Técnico Avenida Rovisco Pais 1, 1049-001 Lisboa, Portugal
(Received 6 May 2008; published 18 July 2008)

The most general supersymmetric seesaw mechanism has too many parameters to be predictive and thus can not be excluded by *any* measurements of lepton flavor violating (LFV) processes. We focus on the simplest version of the type I seesaw mechanism assuming minimal supergravity boundary conditions. We compute branching ratios for the LFV scalar tau decays, $\tilde{\tau}_2 \rightarrow (e, \mu) + \chi_1^0$, as well as loop-induced LFV decays at low energy, such as $l_i \rightarrow l_j + \gamma$ and $l_i \rightarrow 3l_j$, exploring their sensitivity to the unknown seesaw parameters. We find some simple, extreme scenarios for the unknown right-handed parameters, where ratios of LFV branching ratios correlate with neutrino oscillation parameters. If the overall mass scale of the left neutrinos and the value of the reactor angle were known, the study of LFV allows, in principle, to extract information about the so-far unknown right-handed neutrino parameters.

DOI: [10.1103/PhysRevD.78.013006](https://doi.org/10.1103/PhysRevD.78.013006)

PACS numbers: 14.60.Pq, 12.60.Jv, 14.80.Cp

I. INTRODUCTION

Neutrino oscillation experiments have demonstrated that neutrinos are massive particles [1]. With the most recent experimental data by the MINOS [2] and KamLAND [3] collaborations, atmospheric and solar mass-squared differences are now known very precisely and global fits to all neutrino oscillation data [4] also give quite accurate determinations for the corresponding neutrino mixing angles. For the overall mass scale of neutrinos and the third neutrino mixing angle currently only upper limits exist, but considerable progress is expected from future double beta decay [5] and reactor neutrino oscillation [6,7] experiments.

Neutrino masses provide the first experimental signal of physics beyond the standard model (SM). From an experimental point of view, neutrino oscillation data can easily be fitted in very much the same way as the SM accounts for quark masses and mixings, i.e., namely by Dirac neutrino masses. From a theoretical point of view, however, such an ansatz is *ad hoc* since, being electrically neutral, neutrinos are expected to be Majorana particles [8]. Indeed, as noted already in [9], the dimension-five operator,

$$m_\nu = \frac{f}{\Lambda} (HL)(HL), \quad (1)$$

induces *Majorana* masses for neutrinos once the electroweak symmetry breaks. This way the smallness of the neutrino masses can then be attributed to the existence of some lepton number violating scale larger than the electroweak scale. A variety of ways to generate this operator have been suggested. The resulting Majorana neutrino masses can be suppressed either by loop factors, by a large mass scale, by a small scale whose absence enhances the symmetry of theory, or by combinations of these mechanisms [10].

Electroweak scale models, such as, for example, the Zee model [11], the Babu-Zee model [12], supersymmetric models with violation of R parity [13–17], or lepton number violating leptoquark models [18] generate neutrino masses at loop level, resulting in $f \ll 1$ and Λ need not be much larger than m_W . A similar situation arises in models like the inverse seesaw [19]. Such low-scale models have the advantage that the new fields responsible for the generation of neutrino masses may be directly accessible to future accelerator experiments, see for example [20–24].

The most popular mechanism to generate Majorana neutrino masses, however, the celebrated seesaw mechanism [8,25–29] assumes that the lepton number is violated at a very large scale, probably at energies comparable to the grand unification scale. This “classical” version of the

*mahirsch@ific.uv.es

+valle@ific.uv.es

‡porod@physik.uni-wuerzburg.de

§jorge.romao@ist.utl.pt

||albert@cftp.ist.utl.pt

seesaw mechanism, while automatically suppressing neutrino masses without the need for any small prefactor, will unfortunately never be directly testable.

However *indirect* insight into the high-energy world might become possible, if weak scale supersymmetry is realized in nature. Indeed, starting from flavor diagonal soft supersymmetry (SUSY) breaking terms at some high-energy “unification” scale, flavor violation appears at lower energies due to the renormalization group running of the soft breaking parameters [30]. If the (type I) seesaw mechanism is responsible for the observed neutrino masses, the neutrino Yukawa couplings leave their imprint in the slepton mass matrices as shown first in [31]. Flavor off diagonal entries in the neutrino Yukawas then can lead to potentially large lepton flavor violating lepton decays such as $l_i \rightarrow l_j + \gamma$ and $l_i \rightarrow 3l_j$ [32–37] or $\mu - e$ conversion in nuclei [38,39]. In a similar spirit, if supersymmetry is discovered at a future accelerator such as the LHC, one can use measurements of masses and branching ratios of supersymmetric particles to obtain indirect information on the range of allowed seesaw parameters [40–44]. The most general supersymmetric seesaw mechanism has too many parameters to be predictive and thus can not be excluded by *any* measurements of lepton flavor violating (LFV) processes. Within the supersymmetric version of the seesaw measurements of LFV observables outside the neutrino sector allow one to obtain valuable independent information about the seesaw parameters [45]. There are two logical possibilities of how such LFV measurements might be useful. (a) Given the current incomplete knowledge on the light neutrino masses and angles, one could make some simplified assumptions about the right-handed neutrino sector. Then “predictions” for LFV observables as a function of the remaining unknowns for the left-handed light neutrinos result. Or, (b) one could learn about the parameters of the right-handed neutrinos once the most important, but currently unknown light neutrino observables have been measured. While the second option might look more interesting, the time scale for making progress on m_ν , s_{13} , or the Dirac CP phase δ will be long. Worse still, the Majorana phases of the light neutrinos are unlikely to be ever reliably measured. Hence experimental information most likely will be incomplete and measurements of LFV observables will be useful to at least partially reconstruct the seesaw parameters.

In this paper we study lepton flavor violating decays of the scalar tau as well as LFV lepton decays at low energies. We assume minimal supergravity (mSUGRA) boundary conditions and type I seesaw as the origin of neutrino masses and mixings. We compare the sensitivities of low-energy and accelerator measurements and study their dependence on the most important unknown parameters. LFV measurements at accelerators could be argued to be preferable to the low-energy LFV experiments for “reconstructing” seesaw parameters, since from a theoretical point of view they

involve fewer assumptions. However, the absolute values of LFV stau decays and, for example, $\text{Br}(\mu \rightarrow e + \gamma)$ depend very differently on the unknown SUSY spectrum. Whether low-energy LFV or LFV at accelerators yields more insight into the seesaw mechanism can currently therefore not be predicted.

While absolute values of LFV observables depend very strongly on the soft SUSY breaking parameters, it turns out that ratios of LFV branching ratios can be used to eliminate most of the dependence on the unknown spectrum. I.e., ratios such as, for example, $\text{Br}(\tilde{\tau}_2 \rightarrow e + \chi_1^0)/\text{Br}(\tilde{\tau}_2 \rightarrow \mu + \chi_1^0)$ are constants (for fixed neutrino parameters) over large parts of the supersymmetric parameter space and therefore especially suitable to extract information about the seesaw parameters. We therefore study such ratios in detail, first in a useful analytical approximation and then within a full numerical calculation.

The rest of this paper is organized as follows. In the next section, we will recall the basic features of the supersymmetric seesaw mechanism, mSUGRA, and LFV in the slepton sector. Section III then discusses analytical estimates for slepton mixing angles and the corresponding LFV observables. In Sec. IV we present our numerical results before concluding in Sec. V.

II. SETUP: MSUGRA WITH TYPE I SEESAW

In order to fix the notation, let us briefly recall the main features of the seesaw mechanism and mSUGRA. We will consider only the simplest version of the seesaw mechanism here. It consists in extending the particle content of the minimal supersymmetric standard model by three gauge singlet “right-handed” neutrino superfields. The leptonic part of the superpotential is thus given by

$$W = Y_e^{ji} \hat{L}_i \hat{H}_d \hat{E}_j^c + Y_\nu^{ji} \hat{L}_i \hat{H}_u \hat{N}_j^c + M_i \hat{N}_i^c \hat{N}_i^c, \quad (2)$$

where Y_e and Y_ν denote the charged lepton and neutrino Yukawa couplings, while \hat{N}_i^c are the right-handed neutrino superfields with M_i Majorana mass terms of unspecified origin. Since the \hat{N}_i^c are singlets, one can always choose a basis in which the Majorana mass matrix of the right-handed neutrinos is diagonal \hat{M}_R .

Note that LFV arises from supersymmetric as well as from gauge boson loop diagrams, for example, slepton-gaugino exchange loops and W loops involving right-handed neutrino exchange. The former (SUSY-induced LFV) can be described by taking a basis where the Y_e Yukawa coupling matrix is diagonal, its entries fixed by the observed charged lepton masses. This reduces the relevant physical parameters to a total of 21.

While in extended schemes like inverse seesaw [37,39,46] gauge-induced LFV is potentially sizeable, it is negligible in the simplest type I seesaw model, due to the large values of M_i required. Therefore, we focus on such

intrinsically supersymmetric LFV, which can be well characterized Eq. (2) in the unbroken SU(2) limit.

Different parametrizations for the simplest seesaw have been discussed in the literature. The most convenient choice for our calculation is to go to the basis where the charged lepton mass matrix is diagonal. We then have as parameters nine mass eigenstates (three charged leptons, the three light and the three heavy neutrinos). The remaining 12 parameters can be encoded in two matrices V_L and V_R , with three angles and three phases each, which diagonalize Y_ν ,

$$\hat{Y}_\nu = V_R^\dagger Y_\nu V_L. \quad (3)$$

The effective mass matrix of the left-handed neutrinos is given in the usual seesaw approximation as

$$m_\nu = -\frac{v_U^2}{2} Y_\nu^T \cdot M_R^{-1} \cdot Y_\nu. \quad (4)$$

If one of the M_i eigenvalues of the matrix M_R goes to infinity (or the corresponding vector in Y_ν to zero) the corresponding eigenvalue of m_ν (m_i) goes to zero. Since the neutrino mass matrix is complex symmetric, Eq. (4) is diagonalized by [8]

$$\hat{m}_\nu = U^T \cdot m_\nu \cdot U. \quad (5)$$

Inverting the seesaw equation, Eq. (4), allows one to express Y_ν as [47]

$$Y_\nu = \sqrt{2} \frac{i}{v_U} \sqrt{\hat{M}_R R} \sqrt{\hat{m}_\nu} U^\dagger, \quad (6)$$

where \hat{m}_ν is the diagonal matrix with m_i eigenvalues and R in general is a complex orthogonal matrix. Note, that in the special case $R = 1$, Y_ν contains only ‘‘diagonal’’ products $\sqrt{M_i m_i}$. Note that in this approximation the 18 parameters in Y_ν are reduced to 12, which are expressed as six light neutrino mixing angles and phases in the lepton mixing matrix U , the three light neutrino masses in \hat{m}_ν , and the three heavy right-handed neutrino masses in $\sqrt{\hat{M}_R}$.

In the general minimal supersymmetric standard model, LFV off diagonal entries in the slepton mass matrices are free parameters. In order to correlate LFV in the slepton sector with the LFV encoded in Y_ν one must assume some scheme for supersymmetry breaking. We will restrict ourselves here to the case of mSugra, characterized by four continuous and one discrete free parameter, usually denoted as

$$m_0, \quad M_{1/2}, \quad A_0, \quad \tan\beta, \quad \text{Sgn}(\mu). \quad (7)$$

Here, m_0 is the common scalar mass, $M_{1/2}$ the gaugino mass, and A_0 the common trilinear parameter, all defined at the grand unification scale, $M_X \simeq 2 \cdot 10^{16}$ GeV. The remaining two parameters are $\tan\beta = v_U/v_D$ and the sign of the Higgs mixing parameter μ . For reviews on mSugra, see, for example [48,49].

Calculable LFV entries appear in the slepton mass matrices, due to the nontrivial generation structure of the

neutrino Yukawa matrix in Eq. (2), as first pointed out in [31]. In order to determine their magnitude we solve the complete set of renormalization group equations, given in [33,50]. It is however useful for a qualitative understanding, to consider first the simple solutions to the renormalization group equations found in the leading-log approximation [33], given by

$$(\Delta M_{\tilde{L}}^2)_{ij} = -\frac{1}{8\pi^2} (3m_0^2 + A_0^2) (Y_\nu^\dagger L Y_\nu)_{ij} \quad (8)$$

$$(\Delta A_l)_{ij} = -\frac{3}{8\pi^2} A_0 Y_{l_i} (Y_\nu^\dagger L Y_\nu)_{ij} \quad (\Delta M_{\tilde{E}}^2)_{ij} = 0,$$

where only the parts proportional to the neutrino Yukawa couplings have been written. The factor L is defined as

$$L_{kl} = \log\left(\frac{M_X}{M_k}\right) \delta_{kl}. \quad (9)$$

Equation (8) shows that, within the type I seesaw mechanism the right slepton parameters do not run in the leading-log approximation. Thus, LFV scalar decays should be restricted to the sector of left sleptons in practice, apart from left-right mixing effects which could show up in the scalar tau sector. Also note that for the trilinear parameters running is suppressed by charged lepton masses.

Note also that the LFV slepton mass squareds involve a different combination of neutrino Yukawas and right-handed neutrino masses than the left-handed neutrino masses of Eq. (4). In fact, since $(Y_\nu^\dagger L Y_\nu)$ is a Hermitian matrix, it obviously contains only nine free parameters [45], the same number of unknowns as on the right-hand side of Eq. (6), given that in principle all three light neutrino masses, three mixing angles, and three CP phases are potentially measurable.¹

In an ideal world where all low-energy parameters, namely, the three light neutrino masses, three mixings, and three CP violation parameters were known, the remaining parameters entering Eq. (2) could in principle be reconstructed by measuring all entries in $(\Delta M_{\tilde{L}}^2)_{ij}$. This would determine the full set of $18 + 3$ parameters which, to a good approximation, characterize LFV in the minimal type I seesaw. In practice, however, there are two obstacles. (i) Calculability of $(\Delta M_{\tilde{L}}^2)_{ij}$ using Eq. (8) assumes implicitly that there are no threshold effects near the unification scale which destroy the strict proportionality to the parameters m_0 and A_0 [52]. In realistic grand unified theory models this might not be the case. And, (ii) it is not realistic to assume that all entries in $(\Delta M_{\tilde{L}}^2)_{ij}$ can be measured with sufficient accuracy, since (a) the diagonal

¹In practice measuring the unknown angle θ_{13} and the Dirac CP phase requires improved neutrino oscillation studies [51] and will not be an easy task. Even if we are lucky to measure the overall neutrino mass scale in $\beta\beta_{0\nu}$ experiments [5], the Majorana phases contained in U are much harder to determine in practice.

shifts $(\Delta M_{\tilde{L}}^2)_{ii}$ are very small compared to $(M_{\tilde{L}}^2)_{ii}$ (nearly everywhere in the available parameter space) and (b) the determination of the phases required to measure CP -violating LFV observables. The latter does not seem to be a very realistic option either, since, as our numerical results show, one expects only rather low statistics to be available in measurements of LFV slepton decays.

III. ANALYTICAL RESULTS FOR FLAVOR VIOLATING PROCESSES

In this section we present some general formulas describing lepton flavor violation within type I seesaw schemes. We concentrate on the discussion of ratios of LFV branching ratios, since, as mentioned in the introduction, these are most easily connected to the seesaw parameters. As a first approximation we adopt the mass-insertion approximation, neglecting left-right mixing in the slepton mass matrix and taking the leading logs (see, below). We will demonstrate the reliability of our analytical estimates in the next section, where we perform a full numerical calculation of the various LFV branching ratios, which does not rely on any of the approximations discussed in this section.

A. General formulas

The charged slepton mass matrix is a (6, 6) matrix, containing left and right sleptons. Here we concentrate exclusively on the left-slepton sector. Taking into account the discussion given in Sec. II, this is a reasonable first approximation, as can be seen from Eq. (8). The left-slepton mass matrix is diagonalized by a matrix $R^{\tilde{l}}$, which in general can be written as a product of three Euler rotations. However, if the mixing between the different flavor eigenstates is sufficiently small, $R^{\tilde{l}}$ can be approximated as

$$R^{\tilde{l}} \simeq \begin{pmatrix} 1 & \theta_{\tilde{e}\tilde{\mu}} & \theta_{\tilde{e}\tilde{\tau}} \\ -\theta_{\tilde{e}\tilde{\mu}} & 1 & \theta_{\tilde{\mu}\tilde{\tau}} \\ -\theta_{\tilde{e}\tilde{\tau}} & -\theta_{\tilde{\mu}\tilde{\tau}} & 1 \end{pmatrix}, \quad (10)$$

an approximation that corresponds to that employed in the mass-insertion method [31]. In this small-angle approximation each angle can be estimated by the following simple formula

$$\theta_{ij} \simeq \frac{(\Delta M_{\tilde{L}}^2)_{ij}}{(\Delta M_{\tilde{L}}^2)_{ii} - (\Delta M_{\tilde{L}}^2)_{jj}}. \quad (11)$$

LFV decays are directly proportional to the squares of

$$U = \begin{pmatrix} c_{12}c_{13} & s_{12}c_{13} & s_{13}e^{-i\delta} \\ -s_{12}c_{23} - c_{12}s_{23}s_{13}e^{i\delta} & c_{12}c_{23} - s_{12}s_{23}s_{13}e^{i\delta} & s_{23}c_{13} \\ s_{12}s_{23} - c_{12}c_{23}s_{13}e^{i\delta} & -c_{12}s_{23} - s_{12}c_{23}s_{13}e^{i\delta} & c_{23}c_{13} \end{pmatrix} \quad (15)$$

²The inclusion of this factor (and similar corrections for the other low-energy LFV decays) is necessary, since $(r_{kl}^{ij})^2$ relate really partial widths, whereas the measured quantity is usually the branching ratio.

these mixing angles, for example $\text{Br}(\mu \rightarrow e + \gamma) \sim (\theta_{\tilde{e}\tilde{\mu}})^2$ if all angles are small.

Within mSUGRA ratios of LFV branching ratios can then be used to minimize the dependence of observables on SUSY parameters. Consider the case of LFV decays which involve only one generation of sleptons, for example $\text{Br}(\tilde{\tau}_2 \rightarrow e + \chi_1^0)$ and $\text{Br}(\tilde{\tau}_2 \rightarrow \mu + \chi_1^0)$. Taking the ratio of these two decays

$$\frac{\text{Br}(\tilde{\tau}_2 \rightarrow e + \chi_1^0)}{\text{Br}(\tilde{\tau}_2 \rightarrow \mu + \chi_1^0)} \simeq \left(\frac{\theta_{\tilde{e}\tilde{\tau}}}{\theta_{\tilde{\mu}\tilde{\tau}}} \right)^2 \simeq \left(\frac{(\Delta M_{\tilde{L}}^2)_{13}}{(\Delta M_{\tilde{L}}^2)_{23}} \right)^2, \quad (12)$$

i.e., one expects that (a) all the unknown SUSY mass parameters and (b) the denominators of Eq. (11) cancel approximately. The latter should happen practically everywhere in mSUGRA parameter space since $(M_{\tilde{L}}^2)_{ee} \simeq (M_{\tilde{L}}^2)_{\mu\mu}$. This straightforward observation forms the basis for our claim that *ratios of branching ratios* are the theoretically cleanest way to learn about the unknown seesaw parameters. Numerically we have found, that relations similar to Eq. (12) hold also for ratios of observables involving decaying particles of different generations, such as the low-energy ratio $\text{Br}(\mu \rightarrow e + \gamma)/\text{Br}(\tau \rightarrow e + \gamma)$.

To calculate estimates for the different ratios of branching ratios we therefore define

$$r_{kl}^{ij} \equiv \frac{|(\Delta M_{\tilde{L}}^2)_{ij}|}{|(\Delta M_{\tilde{L}}^2)_{kl}|} \quad (13)$$

where the observable quantity is $(r_{kl}^{ij})^2$. Of course, only two of the three possible combinations that can be formed are independent. For example, $\text{Br}(\mu \rightarrow e + \gamma)/\text{Br}(\tau \rightarrow e + \gamma) \simeq (r_{13}^{12})^2 \times \mathcal{R}$. Here, \mathcal{R} is a correction factor taking into account the different total widths of the muon and the tau, $\mathcal{R} = \Gamma_{\tau}/\Gamma_{\mu}$.²

In the leading-log approximation the off diagonal elements of the charged slepton mass matrix are proportional to $(\Delta M_{\tilde{L}}^2)_{ij} \propto ((Y^\nu)^\dagger L(Y^\nu))_{ij}$. Using the parametrization for the Yukawa couplings of Eq. (6) the entries in $(\Delta M_{\tilde{L}}^2)_{ij}$ can be expressed as

$$(\Delta M_{\tilde{L}}^2)_{ij} \propto U_{i\alpha} U_{j\beta}^* \sqrt{m_\alpha} \sqrt{m_\beta} R_{k\alpha}^* R_{k\beta} M_k \log \left(\frac{M_X}{M_k} \right). \quad (14)$$

We can now rewrite Eq. (14) in terms of observables which are more directly related to experiments. In the standard parametrization for the leptonic mixing matrix U is completely analogous to the Cabibbo-Kobayashi-Maskawa matrix and can be written as

where we assumed strict unitarity and neglected the Majorana phases [8], because they do not affect lepton number conserving processes such as the LFV decays we are concerned with here.

Given that neutrino oscillation experiments fix two mass-squared splittings, we can reexpress the three light neutrino masses in terms of one overall neutrino mass scale and the measured quantities Δm_{\odot}^2 and Δm_{A}^2 , where Δm_{\odot}^2 (Δm_{A}^2) is the solar (atmospheric) mass-squared splitting. We will refer to the case of $m_1 \equiv 0$ ($m_3 \equiv 0$) as strict normal (inverse) hierarchy. This choice has the advantage that in both cases $s_{12} \equiv \sin\theta_{\odot}$ and $s_{23} \equiv \sin\theta_a$. Equation (14) can then be written in terms of the measured neutrino angles s_{12} and s_{23} , the measured neutrino mass-squared splittings, plus the so far unknown overall neutrino mass scale m_{ν} and the reactor neutrino angle $s_{13} \equiv s_R$. If the latter were measured, one could extract information on the right-handed neutrino mass scale and/or the matrix R from Eq. (14). Conversely, we could learn about m_{ν} and s_{13} from measurements of LFV decays, making some assumptions about the scale M_R and the possible textures of the Yukawa couplings that determine M_R and R .

B. Degenerate right-handed neutrinos

In this subsection we will assume that the three right-handed neutrinos are degenerate. This simplifying ansatz allows us to study the sensitivity with a single mass-scale parameter associated with the neutrino mass generation via the type I seesaw mechanism. This ansatz can be theoretically motivated in the framework of some flavor symmetries, for example A_4 [53]. In the special case that the matrix R is real, Eq. (14) reduces to

$$\begin{aligned}
 (\Delta M_{\bar{L}}^2)_{12} &\propto c_{12}c_{13}(-s_{12}c_{23} - c_{12}s_{23}s_{13}e^{-i\delta})z_1 \\
 &\quad + s_{12}c_{13}(c_{12}c_{23} - s_{12}s_{23}s_{13}e^{-i\delta})z_2 \\
 &\quad + s_{23}c_{13}s_{13}e^{-i\delta}z_3 \\
 (\Delta M_{\bar{L}}^2)_{13} &\propto c_{12}c_{13}(s_{12}s_{23} - c_{12}c_{23}s_{13}e^{-i\delta})z_1 \\
 &\quad + s_{12}c_{13}(-c_{12}s_{23} - s_{12}c_{23}s_{13}e^{-i\delta})z_2 \\
 &\quad + c_{23}c_{13}s_{13}e^{-i\delta}z_3 \\
 (\Delta M_{\bar{L}}^2)_{23} &\propto (s_{12}s_{23} - c_{12}c_{23}s_{13}e^{-i\delta}) \\
 &\quad \times (-s_{12}c_{23} - c_{12}s_{23}s_{13}e^{i\delta})z_1 \\
 &\quad + (-c_{12}s_{23} - s_{12}c_{23}s_{13}e^{-i\delta}) \\
 &\quad \times (c_{12}c_{23} - s_{12}s_{23}s_{13}e^{i\delta})z_2 + s_{23}c_{23}c_{13}^2z_3
 \end{aligned} \tag{16}$$

where

$$z_i \equiv m_i M_i \log\left(\frac{M_X}{M_i}\right). \tag{17}$$

For this degenerate right-handed neutrino ansatz the combination $M_i \log\left(\frac{M_X}{M_i}\right)$ becomes an overall factor, which can

be taken out from Eq. (14), since it cancels upon taking ratios. I.e., for degenerate right-handed neutrinos one may simply make the replacement $z_i \rightarrow m_i$ in Eq. (16).

As a starting approximation for the following estimates, let us assume that the lepton mixing matrix has the exact tribimaximal (TBM) form [54]

$$U = U_{\text{TBM}} = \begin{pmatrix} \sqrt{\frac{2}{3}} & \frac{1}{\sqrt{3}} & 0 \\ -\frac{1}{\sqrt{6}} & \frac{1}{\sqrt{3}} & \frac{1}{\sqrt{2}} \\ \frac{1}{\sqrt{6}} & -\frac{1}{\sqrt{3}} & \frac{1}{\sqrt{2}} \end{pmatrix}. \tag{18}$$

As is well-known, Eq. (18) is an excellent first-order approximation to the measured neutrino mixing angles [4]. With this assumption the ratios of the off diagonal elements of the charged slepton mass matrix are simply given by

$$r_{13}^{12} = 1 \quad r_{23}^{12} = r_{23}^{13} = \frac{2(m_2 - m_1)}{|3m_3 - 2m_2 - m_1|}. \tag{19}$$

As Eq. (19) shows r_{23}^{12} and r_{23}^{13} depend on mass-squared splittings and on the overall neutrino mass scale, i.e., also on the unknown neutrino mass hierarchy. In the case of strict normal hierarchy (SNH, $m_1 \equiv 0$)

$$r_{23}^{12} = r_{23}^{13} = \frac{2\sqrt{\alpha}}{3\sqrt{1+\alpha} - 2\sqrt{\alpha}} \tag{20}$$

where $\alpha \equiv \frac{\Delta m_{\odot}^2}{|\Delta m_{\text{A}}^2|}$, while for the case of strict inverse hierarchy (SIH, $m_3 \equiv 0$)

$$r_{23}^{12} = r_{23}^{13} = \frac{2(1 - \sqrt{1 - \alpha})}{2 + \sqrt{1 - \alpha}}. \tag{21}$$

Finally, for quasidegenerate (QD) neutrinos, defined as $\sqrt{\Delta m_{\text{A}}^2} \ll m_{\nu}$, one finds

$$r_{23}^{12} = r_{23}^{13} \simeq \frac{2\alpha}{3\sigma_{\text{A}} + \alpha} \tag{22}$$

where σ_{A} is the sign of the atmospheric mass splitting

$$\sigma_{\text{A}} \equiv \frac{\Delta m_{\text{A}}^2}{|\Delta m_{\text{A}}^2|}. \tag{23}$$

Note that σ_{A} equals +1 (−1) for normal (inverse) hierarchy. Thus QD neutrinos with normal (QDNH) or inverse hierarchy (QDIH) lead formally to different results. However, this difference is numerically not relevant, once uncertainties are taken into account.

Figure 1 shows the ratio $(r_{23}^{13})^2$ versus the neutrino mass m_1 in eV for normal (inverse) hierarchy. The figure demonstrates the importance of the absolute neutrino mass scale for $(r_{23}^{13})^2$. In the most general case one must use

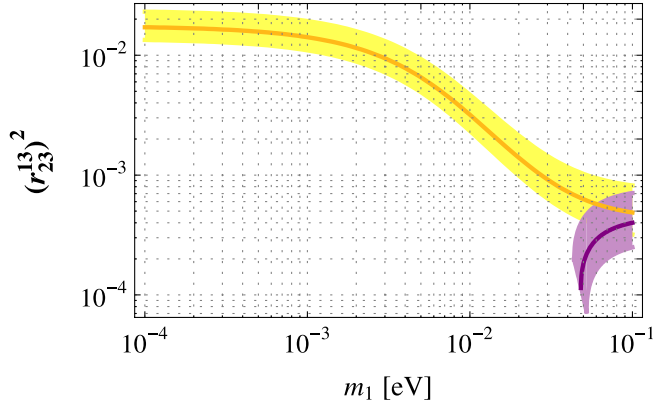


FIG. 1 (color online). Ratio $(r_{23}^{13})^2$ versus the neutrino mass m_1 in eV. The light/yellow (dark/violet) band is for the case of normal (inverse) hierarchy. The width of the band indicates the uncertainty due to the currently allowed 3σ C.L. ranges for Δm_A^2 and Δm_δ^2 . The calculation assumes exact tribimaximal mixing for the left-handed neutrinos.

Eqs. (13) and (16). However, for $s_{13} = 0$ the explicit dependence of the ratios of the off diagonal elements of the charged slepton mass-squared matrix on the other

neutrino angles matrix follows rather simple expressions

$$\begin{aligned} r_{13}^{12} &= \frac{c_{23}}{s_{23}}, \\ r_{23}^{12} &= \frac{1}{s_{23}} s_{12} c_{12} \frac{m_2 - m_1}{|m_3 - c_{12}^2 m_2 - s_{12}^2 m_1|}, \\ r_{23}^{13} &= \frac{1}{c_{23}} s_{12} c_{12} \frac{m_2 - m_1}{|m_3 - c_{12}^2 m_2 - s_{12}^2 m_1|}. \end{aligned} \quad (24)$$

Figures 2 and 3 show the dependence of the square ratios $(r_{kl}^{ij})^2$ as a function of s_{13}^2 for the different extreme cases of SNH and SIH as well as QDNH and QDIH, for two choices of the Dirac phase $\delta = 0, \pi$. These ratios $(r_{kl}^{ij})^2$ depend strongly on s_{13}^2 . Note from Eq. (16) that for $\tan^2 \theta_A = 1$, $(r_{23}^{12})^2$ and $(r_{23}^{13})^2$ are invariant under the exchange of $\delta = 0 \leftrightarrow \delta = \pi$. If $\tan^2 \theta_A \neq 1$, this symmetry is broken, but always one of the two ratios r_{23}^{12} and r_{23}^{13} is guaranteed to be nonvanishing regardless of the value of s_{13} . A nonzero measurement of both ratios would therefore in principle contain information on both s_{13} and δ (if right-handed neutrinos are degenerate).

Figure 3 shows also that the cases QDNH and QDIH are also symmetric under the simultaneous exchange of

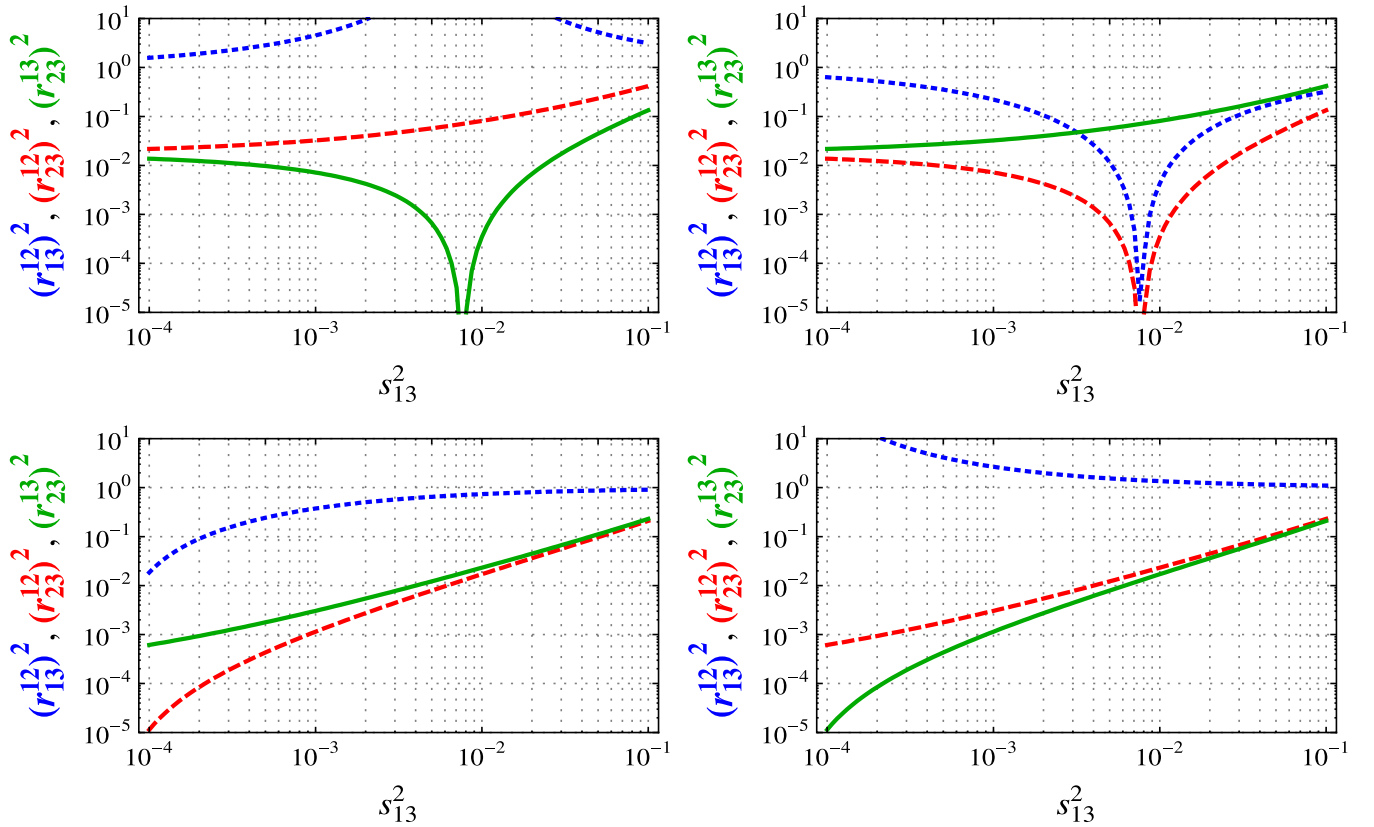


FIG. 2 (color online). Square ratios $(r_{13}^{12})^2$ (blue line/dotted line), $(r_{23}^{12})^2$ (red line/dashed line), and $(r_{23}^{13})^2$ (green line/full line) versus s_{13}^2 for SNH (upper panels), SIH (lower panels) for $\delta = 0$ (left panels) and $\delta = \pi$ (right panels). The plots assume that the heavy neutrinos are degenerate. The other light neutrino parameters have been fixed to their b.f.p. values. Note from Eq. (16), that for $\tan^2 \theta_A = 1$, $(r_{23}^{12})^2$, and $(r_{23}^{13})^2$ are symmetric under the exchange of $\delta = 0 \leftrightarrow \delta = \pi$.

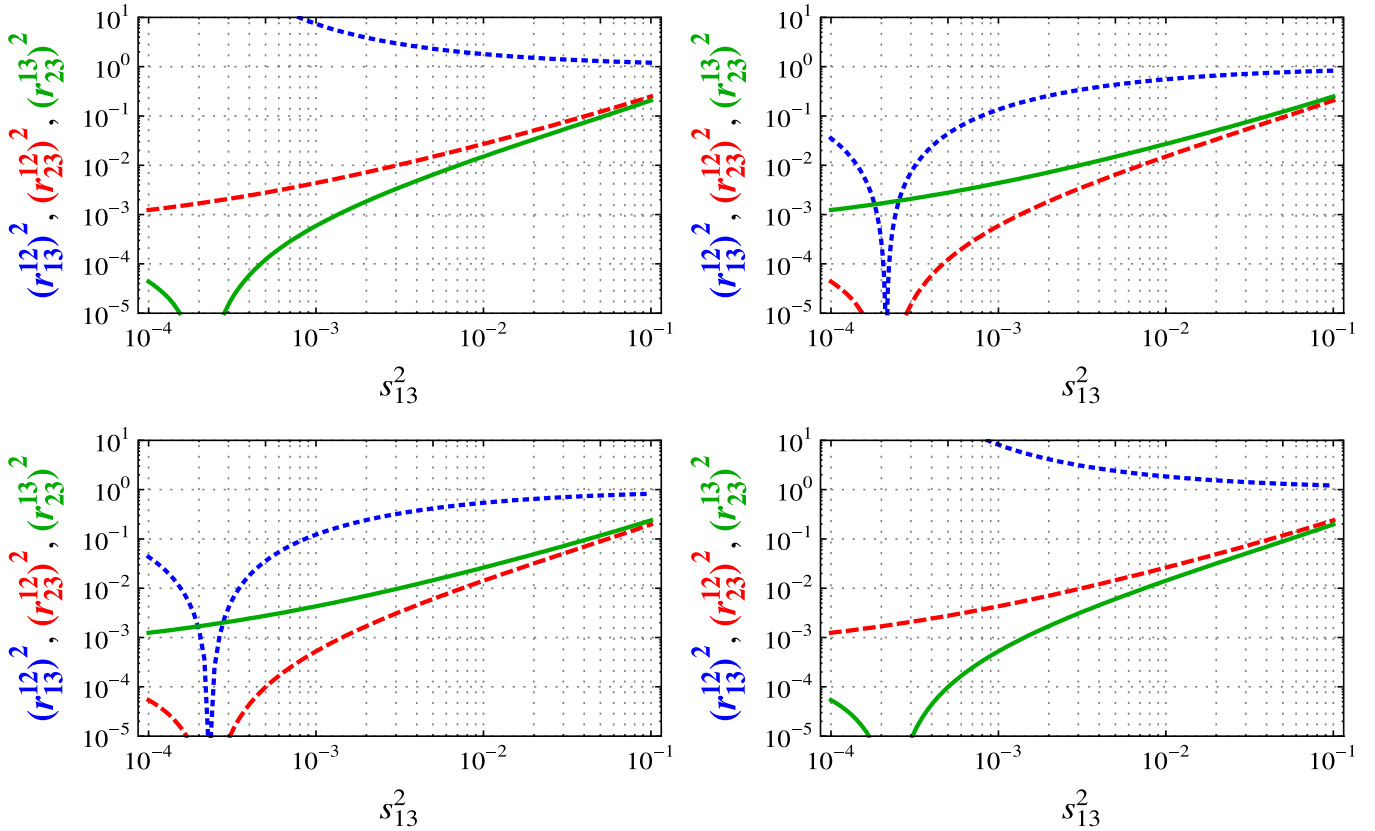


FIG. 3 (color online). As Fig. 2, but for the limit of quasidegenerate light neutrinos. Square ratios $(r_{13}^{12})^2$ (blue line/dotted line), $(r_{23}^{12})^2$ (red line/dashed line), and $(r_{23}^{13})^2$ (green line/full line) versus s_{13}^2 for QDNH (upper panels), QDIH (lower panels) for $\delta = 0$ (left panels) and $\delta = \pi$ (right panels).

TABLE I. The parameters r_{kl}^{ij} are given for several values of neutrino oscillation parameters. SNH and SIH are strict normal and strict inverted hierarchy of neutrino masses, respectively. Rows labeled as TBM assume the TBM values for θ_{12} and θ_{23} and the neutrino mass splittings have been fixed to their b.f.p. values taken from [4]. Rows labeled as 3σ take into account current allowed 3σ ranges of neutrino oscillation parameters. In the first column, θ_{13} has been fixed to its TBM value ($s_{13} = 0$), while in the second and third columns s_{13} has been fixed to its maximum allowed value: $(s_{13}^{\max})^2 = 0.050$ at 3σ C.L. and the Dirac phase is fixed to $\delta = 0$ and $\delta = \pi$, respectively.

			$s_{13} = 0$	$s_{13} = s_{13}^{\max}, \delta = 0$	$s_{13} = s_{13}^{\max}, \delta = \pi$
SNH	TBM	$(r_{13}^{12})^2$	1.0	5.2	1.9×10^{-1}
		$(r_{23}^{12})^2$	1.7×10^{-2}	2.3×10^{-1}	4.4×10^{-2}
		$(r_{23}^{13})^2$	1.7×10^{-2}	4.4×10^{-2}	2.3×10^{-1}
	3σ	$(r_{13}^{12})^2$	[0.49, 1.9]	[1.8, 35]	$[0.33, 5.7] \times 10^{-1}$
		$(r_{23}^{12})^2$	$[0.91, 3.6] \times 10^{-2}$	$[2.0, 3.2] \times 10^{-1}$	$[0.96, 12] \times 10^{-2}$
		$(r_{23}^{13})^2$	$[0.92, 3.7] \times 10^{-2}$	$[0.87, 11] \times 10^{-2}$	$[2.0, 3.2] \times 10^{-1}$
SIH	TBM	$(r_{13}^{12})^2$	1.0	8.7×10^{-1}	1.1
		$(r_{23}^{12})^2$	1.1×10^{-4}	9.7×10^{-2}	1.1×10^{-1}
		$(r_{23}^{13})^2$	1.1×10^{-4}	1.1×10^{-1}	9.7×10^{-2}
	3σ	$(r_{13}^{12})^2$	[0.49, 1.9]	$[4.2, 18] \times 10^{-1}$	[0.57, 2.5]
		$(r_{23}^{12})^2$	$[0.47, 3.2] \times 10^{-4}$	$[6.9, 15] \times 10^{-2}$	$[0.85, 1.7] \times 10^{-1}$
		$(r_{23}^{13})^2$	$[0.48, 3.3] \times 10^{-4}$	$[0.83, 1.6] \times 10^{-1}$	$[6.8, 15] \times 10^{-2}$

TABLE II. The parameters r_{kl}^{ij} are given for several values of neutrino oscillation parameters. QD stands for the quasidegenerate limit, while NH (IH) indicate that the neutrino hierarchy is normal (inverse). The neutrino parameters have been varied in the same way as in Table I.

			$s_{13} = 0$	$s_{13} = s_{13}^{\max}, \delta = 0$	$s_{13} = s_{13}^{\max}, \delta = \pi$
QDNH	TBM	$(r_{13}^{12})^2$	1.0	1.3	7.7×10^{-1}
		$(r_{23}^{12})^2$	4.4×10^{-4}	1.2×10^{-1}	9.4×10^{-2}
		$(r_{23}^{13})^2$	4.4×10^{-4}	9.4×10^{-2}	1.2×10^{-1}
	3σ	$(r_{13}^{12})^2$	[0.49, 1.9]	[0.63, 3.0]	$[3.5, 17] \times 10^{-1}$
		$(r_{23}^{12})^2$	$[1.8, 12] \times 10^{-4}$	$[0.94, 1.8] \times 10^{-1}$	$[6.2, 15] \times 10^{-2}$
		$(r_{23}^{13})^2$	$[1.8, 12] \times 10^{-4}$	$[6.1, 15] \times 10^{-2}$	$[0.93, 1.8] \times 10^{-1}$
QDIH	TBM	$(r_{13}^{12})^2$	1.0	7.6×10^{-1}	1.3
		$(r_{23}^{12})^2$	4.6×10^{-4}	8.9×10^{-2}	1.2×10^{-1}
		$(r_{23}^{13})^2$	4.6×10^{-4}	1.2×10^{-1}	8.9×10^{-2}
	3σ	$(r_{13}^{12})^2$	[0.49, 1.9]	$[3.4, 16] \times 10^{-1}$	[0.64, 3.1]
		$(r_{23}^{12})^2$	$[1.9, 13] \times 10^{-4}$	$[5.9, 15] \times 10^{-2}$	$[0.89, 1.8] \times 10^{-1}$
		$(r_{23}^{13})^2$	$[1.9, 13] \times 10^{-4}$	$[0.88, 1.7] \times 10^{-1}$	$[5.8, 14] \times 10^{-2}$

$\delta = 0 \leftrightarrow \delta = \pi$ and QDNH \leftrightarrow QDIH, for the case of $\tan^2 \theta_A = 1$. This symmetry is broken in all cases for $\tan^2 \theta_A \neq 1$, as seen from the numerical values given in Tables I and II. Tables I and II show numerical values for r_{kl}^{ij} for the extreme cases of SNH, SIH, QDNH, and QDIH for various different choices of neutrino parameters. In the rows labeled as TBM, we have used the TBM values for θ_{12} and θ_{23} and the neutrino mass splittings have been fixed to their best-fit values taken from Ref. [4]. In the rows labeled as 3σ , we take into account the experimentally allowed 3σ ranges for neutrino oscillation parameters: $s_{12}^2 = 0.26 - 0.40$, $s_{23}^2 = 0.34 - 0.67$, $\Delta m_{\odot}^2 = (7.1 - 8.3) \times 10^{-5} \text{ eV}^2$, and $\Delta m_A^2 = (2.0 - 2.8) \times 10^{-3} \text{ eV}^2$. In the first column, θ_{13} has been fixed to its TBM value ($s_{13} = 0$), while in the second and third columns s_{13} has been fixed to s_{13}^{\max} , which is the experimentally allowed maximum value: $(s_{13}^{\max})^2 = 0.050$ at 3σ C.L. In the second column, the Dirac phase is fixed to $\delta = 0$, while in the third column $\delta = \pi$. Note that, as already mentioned, these estimates are valid in the small mixing limit and hence these values are indicative only.

C. Right-handed neutrinos strongly hierarchical

One can consider the case of degenerate right-handed neutrinos to be just one extreme limit in a continuum of possibilities. The opposite extreme case would then be to assume right-handed neutrinos are strongly hierarchical. Note that here we make the important assumption that the matrix R is the identity.

1. Dominant M_1

If M_1 is the heaviest mass eigenvalue, the leading terms for the off diagonal slepton masses are (in case $m_1 \neq 0$)

$$\begin{aligned}
 (\Delta M_L^2)_{12} &\propto c_{13}c_{12}(s_{12}c_{23} + s_{13}e^{-i\delta}c_{12}s_{23}) \\
 (\Delta M_L^2)_{13} &\propto c_{13}c_{12}(s_{12}s_{23} - s_{13}e^{-i\delta}c_{12}c_{23}) \\
 (\Delta M_L^2)_{23} &\propto s_{12}^2s_{23}c_{23} - s_{13}s_{12}c_{12}(e^{-i\delta}c_{23}^2 - e^{i\delta}s_{23}^2) \\
 &\quad - s_{13}^2c_{12}^2s_{23}c_{23}.
 \end{aligned} \tag{25}$$

For the special case of $s_{13} = 0$, the ratios simplify to $r_{13}^{12} = \frac{c_{23}}{s_{23}}$, $r_{23}^{12} = \frac{c_{12}}{s_{12}s_{23}}$, and $r_{23}^{13} = \frac{c_{12}}{s_{12}c_{23}}$. Note the large difference in the numerical values compared to the case of degenerate right-handed neutrinos. Here, for example, for $s_{13} = 0$ one finds $(r_{23}^{13})^2 = 4$, whereas in the case of degenerate right-handed neutrinos one obtains $(r_{23}^{13})^2 = 0.017$ [best fit point (b.f.p.) values for Δm_{\odot}^2 and Δm_A^2]. For nonzero values of s_{13} Fig. 4 shows that $(r_{kl}^{ij})^2$ depend to a much lesser degree on s_{13} than for the case of degenerate right-handed neutrinos. Especially, note that for the case of M_1 dominance considered here none of the $(r_{kl}^{ij})^2$ vanish in the allowed range of s_{13} . Numerical values for extreme values of s_{13} are summarized in Table III.

2. Dominant M_2

If M_2 is the heaviest mass eigenvalue, the dominant terms for the off diagonal slepton masses are

$$\begin{aligned}
 (\Delta M_L^2)_{12} &\propto c_{13}s_{12}(c_{12}c_{23} - s_{13}e^{-i\delta}s_{12}s_{23}) \\
 (\Delta M_L^2)_{13} &\propto c_{13}s_{12}(c_{12}s_{23} + s_{13}e^{-i\delta}s_{12}c_{23}) \\
 (\Delta M_L^2)_{23} &\propto c_{12}^2s_{23}c_{23} + s_{13}s_{12}c_{12}(e^{-i\delta}c_{23}^2 - e^{i\delta}s_{23}^2) \\
 &\quad - s_{13}^2s_{12}^2s_{23}c_{23}.
 \end{aligned} \tag{26}$$

For the special case of $s_{13} = 0$, the ratios simplify to $r_{13}^{12} = \frac{c_{23}}{s_{23}}$, $r_{23}^{12} = \frac{s_{12}}{c_{12}s_{23}}$, and $r_{23}^{13} = \frac{s_{12}}{c_{12}c_{23}}$. Here, for example, for $s_{13} = 0$ one finds $(r_{23}^{13})^2 = 1$, whereas for the case of M_1

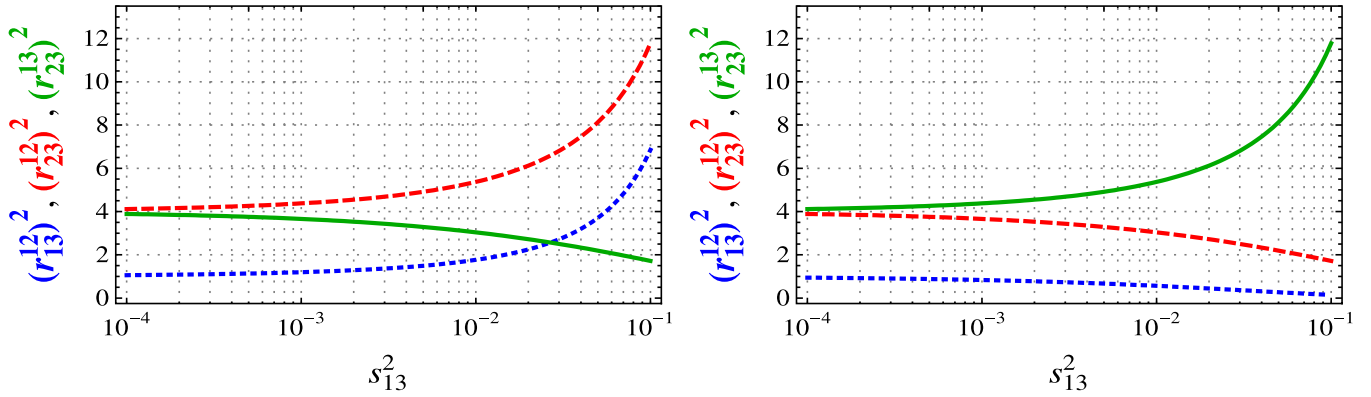


FIG. 4 (color online). Square ratios $(r_{13}^{12})^2$ (blue line/dotted line), $(r_{23}^{12})^2$ (red line/dashed line), and $(r_{23}^{13})^2$ (green line/full line) versus s_{13} for $\delta = 0$ (left panel) and $\delta = \pi$ (right panel) for the case of M_1 being dominant. The remaining neutrino parameters have been fixed to their b.f.p. values.

being dominant this quantity is expected to be $(r_{23}^{13})^2 = 4$. Figure 5 shows the $(r_{kl}^{ij})^2$ as a function of s_{13}^2 for the M_2 dominance case. Again the dependence on s_{13} is weaker than in the case of degenerate right-handed neutrinos. As in the previous case $(r_{kl}^{ij})^2$ never vanishes in the allowed range of s_{13}^2 . Finally, the numerical values also differ from the ones found for the case of M_1 dominance. A summary of numerical values for extreme values of s_{13} is given in Table III.

3. Dominant M_3

If terms proportional to M_3 give the leading contribution one finds

$$\begin{aligned}
 (\Delta M_L^2)_{12} &\propto s_{13} e^{-i\delta} c_{13} s_{23} \\
 (\Delta M_L^2)_{13} &\propto s_{13} e^{-i\delta} c_{13} c_{23} \\
 (\Delta M_L^2)_{23} &\propto c_{13}^2 s_{23} c_{23}.
 \end{aligned}
 \tag{27}$$

TABLE III. The parameters r_{kl}^{ij} are given for several values of neutrino oscillation parameters. Each row labeled as M_i is calculated assuming the contribution from neutrino with mass M_i is dominant. Neutrino oscillation parameters have been varied as in Table I. Notice that the row for dominant M_3 gives the same numerical result for the Dirac phase $\delta = 0$ and $\delta = \pi$.

			$s_{13} = 0$	$s_{13} = s_{13}^{\max}, \delta = 0$	$s_{13} = s_{13}^{\max}, \delta = \pi$
M_1	TBM	$(r_{13}^{12})^2$	1.0	3.7	2.7×10^{-1}
		$(r_{23}^{12})^2$	4.0	8.1	2.2
		$(r_{23}^{13})^2$	4.0	2.2	8.1
	3σ	$(r_{13}^{12})^2$	[0.49, 1.9]	[1.5, 14]	$[0.66, 6.6] \times 10^{-1}$
		$(r_{23}^{12})^2$	[2.2, 8.4]	[3.3, 35]	[1.5, 3.4]
		$(r_{23}^{13})^2$	[2.3, 8.6]	[1.5, 35]	[3.3, 38]
M_2	TBM	$(r_{13}^{12})^2$	1.0	5.3×10^{-1}	1.9
		$(r_{23}^{12})^2$	1.0	7.1×10^{-1}	1.3
		$(r_{23}^{13})^2$	1.0	1.3	7.1×10^{-1}
	3σ	$(r_{13}^{12})^2$	[0.49, 1.9]	$[2.1, 11] \times 10^{-1}$	[0.85, 4.5]
		$(r_{23}^{12})^2$	[0.52, 2.0]	$[4.2, 12] \times 10^{-1}$	[0.61, 3.4]
		$(r_{23}^{13})^2$	[0.53, 2.0]	[0.62, 3.5]	$[4.2, 12] \times 10^{-1}$
M_3	TBM		$s_{13} = 0$	$s_{13} = s_{13}^{\max}$	
		$(r_{13}^{12})^2$...	1.0	
		$(r_{23}^{12})^2$	0.0	1.1×10^{-1}	
	3σ	$(r_{23}^{13})^2$	0.0	1.1×10^{-1}	
		$(r_{13}^{12})^2$...	[0.52, 2.0]	
		$(r_{23}^{12})^2$	0.0	$[0.80, 1.6] \times 10^{-1}$	
		$(r_{23}^{13})^2$	0.0	$[0.79, 1.5] \times 10^{-1}$	

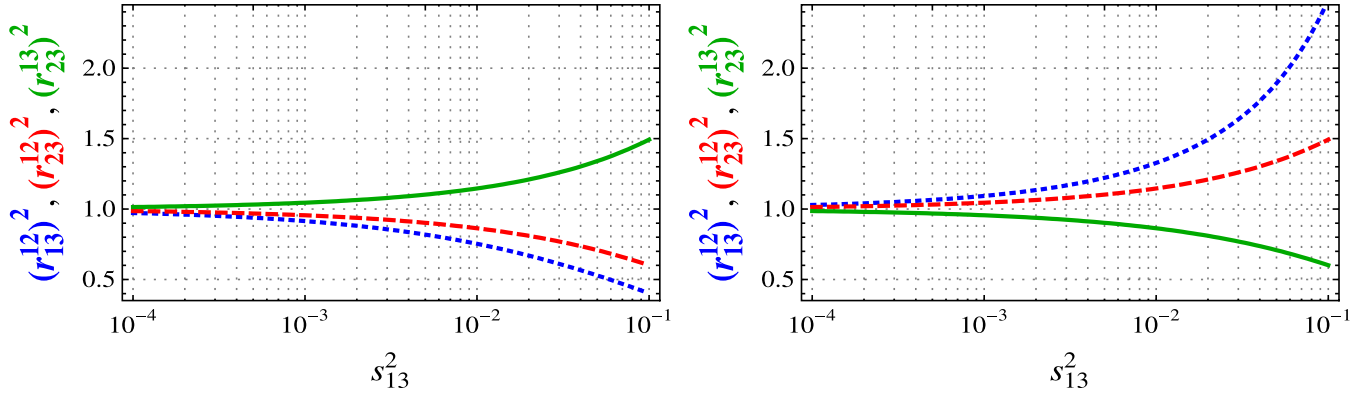


FIG. 5 (color online). Square ratios $(r_{13}^{12})^2$ (blue line/dotted line), $(r_{23}^{12})^2$ (red line/dashed line), and $(r_{23}^{13})^2$ (green line/full line) versus s_{13} for $\delta = 0$ (left panel) and $\delta = \pi$ (right panel) in the case where M_2 is dominant. The other neutrino parameters have been fixed to their b.f.p. values.

For the special case of $s_{13} = 0$, one finds that $r_{23}^{12} = r_{23}^{13} = 0$, otherwise both ratios are proportional to s_{13} . These numerical values allow us to distinguish the M_3 dominance case from the previous hierarchical cases already discussed. Numerical values for extreme values of s_{13} are summarized in Table III.

IV. NUMERICAL RESULTS

The analytical results presented above allow us to estimate ratios of branching ratios for LFV decays. For absolute values of the branching ratios, as well as for cross-checking the reliability of the analytical estimates, one must resort to a numerical calculation. In this section we present results of such a numerical calculation. All results presented below have been obtained with the lepton flavor violating version of the program package SPHENO [55]. For definiteness we will present results only for the mSugra “standard points” SPS3 [56] and SPS1a’ [57], taken as reference examples. However, we have checked with a number of other points that our results for ratios of branching ratios are generally valid. SPS1a’ [57] is a typical point in the “bulk” region for SUSY dark matter. It is a slightly modified version of the original SPS1a point of [56], which gives better agreement with the latest constraints from cold dark matter abundance. It has a relatively light slepton spectrum, i.e., left sleptons around 200 GeV. SPS3 [56] is a point in the coannihilation region for SUSY dark matter. Left sleptons in this point are heavier than in SPS1a’, i.e., they have masses around 350 GeV. We have chosen these two points to show the complementarity between low-energy searches for LFV and LFV scalar tau decays at the LHC, see also the discussion below.

Our numerical procedure to fit the neutrino masses is as follows. Inverting the seesaw equation, see Eq. (4), one can get a first guess of the Yukawa couplings for any fixed values of the light neutrino masses and mixing angles as a function of the corresponding right-handed neutrino masses. We then run numerically the renormalization

group equations taking into account all flavor structures in matrix form. We integrate out every right-handed neutrino and its superpartner at the scale corresponding to its mass and calculated the corresponding contribution to the dimension-five operator which is evaluated to the electro-weak scale. This way we obtain the exact neutrino masses and mixing angles for this first guess. The difference between the results obtained numerically and the input numbers is then minimized in an iterative procedure until convergence is achieved. As is well-known neutrino masses and mixing angles run very little, if physical light neutrino masses are hierarchical [58]. Thus, barring the exceptional case where neutrinos become very degenerate, one usually reaches numerical convergence very fast. For degenerate left neutrinos convergence from first guess to exact results can be slow, especially for relatively large values for the right-handed neutrino masses, which require larger Yukawa coupling constants. In this case we used a numerical fit procedure [59] based on the program MINUIT.³

In the following two subsections we present numerical results first for the case of degenerate right-handed neutrinos, then for the case(s) of very hierarchical right-handed neutrinos. We have checked numerically that, as expected from Eq. (8), right sleptons have small branching ratios for LFV final states. Thus, the discussion concentrates on the decays of the “left” staus $\tilde{\tau}_2 \simeq \tilde{\tau}_L$.

A. Degenerate right-handed neutrinos

In this subsection we still adopt the simplifying ansatz that $R = 1$, see Eq. (6). Two examples for hierarchical light neutrinos are shown in Fig. 6 and 7. Figure 6 has the mSugra parameters fixed to the standard values SPS1a’ [56,57], while Fig. 7 corresponds to SPS3 [56]. The neutrino oscillation data are fitted for the SNH case where

³Minimization package from the CERN Program Library, documentation can be found at <http://cernlib.web.cern.ch/cernlib/>.

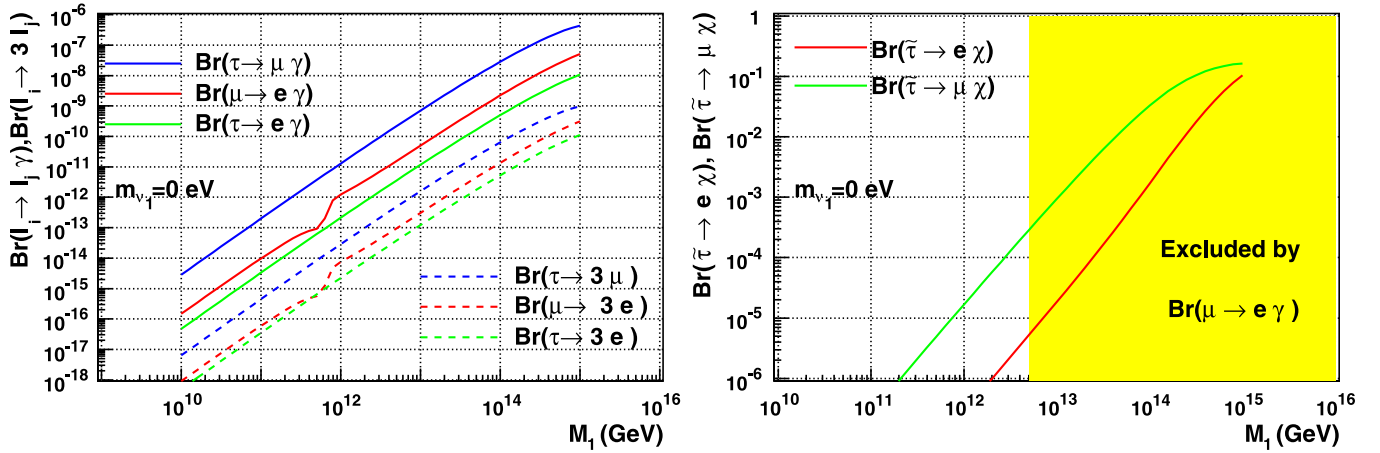


FIG. 6 (color online). Branching ratios for $l_i \rightarrow l_j + \gamma$ and $l_i \rightarrow 3l_j$ (left) and $\tilde{\tau}_2 \rightarrow e + \chi_1^0$ and $\tilde{\tau}_2 \rightarrow \mu + \chi_1^0$ (right) for the standard point SPS1a' versus M_R , assuming degenerate right-handed neutrinos. Neutrino oscillation parameters have been fixed to the best-fit values for Δm_{21}^2 and Δm_{31}^2 , with exact tribimaximal neutrino angles. We also set $m_1 = 0$. The colored region in the right-side plot is excluded from the current experimental limit on $\text{Br}(\mu \rightarrow e + \gamma)$. Thus, one expects for SPS1a' only very small branching ratios for LFV scalar tau decays (compare to Fig. 7).

$m_1 = 0$ with exact tribimaximal mixing. The plot on the left panel shows low-energy lepton flavor violating decay branching ratios for $l_i \rightarrow l_j + \gamma$ and $l_i \rightarrow 3l_j$, while the one on the right panel gives LFV stau ($\tilde{\tau}_2$) decay branching ratios as a function of the right-handed neutrino mass scale $M_1 = M_R$.

As expected, all LFV processes show a strong dependence on M_R . This can be straightforwardly understood from Eqs. (4) and (8). Keeping the light neutrino masses constant ΔM_L^2 are proportional to $M_R \log M_R$, thus all LFV branching ratios grow as $(M_R \log M_R)^2$. As the figures show, as long as M_R is not too large, all lepton flavor violating processes show the same dependence on M_R . Ratios of branching ratios follow very nicely the corresponding analytically calculated ratios for $(r_{kl}^{ij})^2$, once the

corresponding correction factors are taken into account for the low-energy observables. As is well-known [35,39,60], for most parts of the mSugra parameter space one expects

$$\frac{\text{Br}(l_i \rightarrow 3l_j)}{\text{Br}(l_i \rightarrow l_j + \gamma)} \simeq \frac{\alpha}{3\pi} \left(\log \left(\frac{m_{l_i}^2}{m_{l_j}^2} \right) - \frac{11}{4} \right), \quad (28)$$

thus the photonic penguin diagram dominates the three-lepton decay modes $l_i \rightarrow 3l_j$.

Figures 6 and 7 do indeed confirm the validity of this approximation. Only at large values of M_R one observes some deviations from the analytical estimates. The reason for this departure is that in this parameter range the small-angle approximation no longer holds, as can be seen from the absolute values for the decay $\text{Br}(\tilde{\tau}_2 \rightarrow \mu + \chi_1^0)$, which

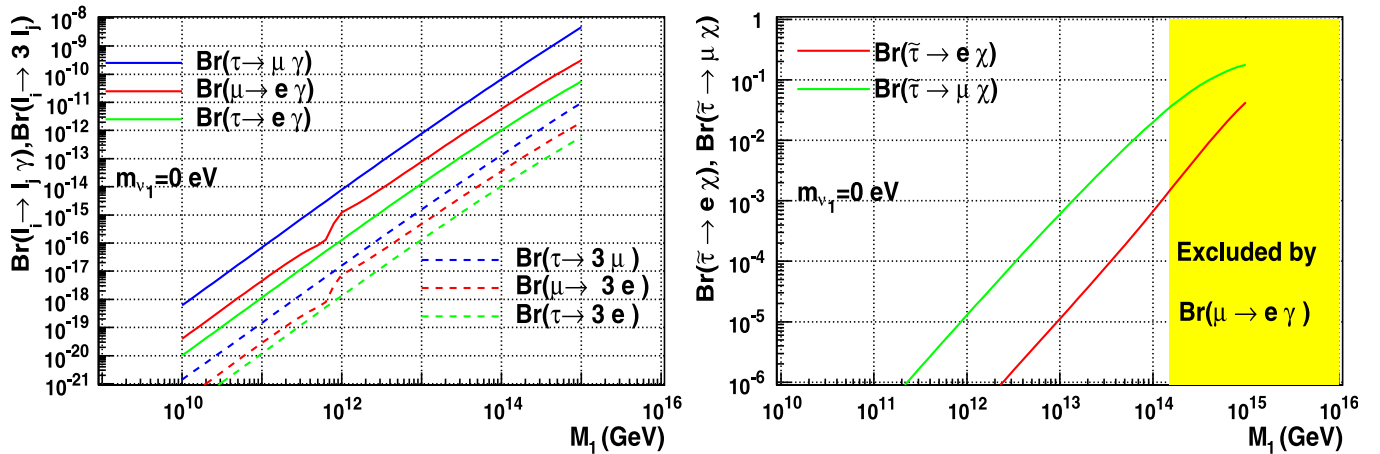


FIG. 7 (color online). Same as Fig. 6, but for the mSugra standard point SPS3. In this point the constraints on the LFV $\tilde{\tau}_2$ decays from the upper limit on $\mu \rightarrow e + \gamma$ are much less severe than for SPS1a'. As a result $\text{Br}(\tilde{\tau}_2 \rightarrow \mu + \chi_1^0)$ could be as large as several percent with all low-energy constraints fulfilled.

can reach more than 10% for $M_R \geq 10^{14}$ GeV. However, Figs. 6 and 7 also show how the LFV $\tilde{\tau}_2$ decays are strongly constrained by low-energy data. For the degenerate right-handed neutrino case shown here (and for $s_{13} = 0$), independent of the mSugra parameters $\text{Br}(\mu \rightarrow e + \gamma)$ is the most important constraint. Applying the current experimental limit on $\text{Br}(\mu \rightarrow e + \gamma)$ of $\text{Br}(\mu \rightarrow e + \gamma) \leq 1.2 \times 10^{-11}$ [61], the branching ratio for $\text{Br}(\tilde{\tau}_2 \rightarrow \mu + \chi_1^0)$ is expected to lie below 10^{-3} for SPS1a', whereas it can reach several percent in case of SPS3. Note that in the range of M_R not excluded by the limit on $\text{Br}(\mu \rightarrow e + \gamma)$ the ratio $\text{Br}(\tilde{\tau}_2 \rightarrow e + \chi_1^0)/\text{Br}(\tilde{\tau}_2 \rightarrow \mu + \chi_1^0)$ follows very well the analytical estimate of Eq. (20). The huge difference in the upper limit for $\text{Br}(\tilde{\tau}_2 \rightarrow \mu + \chi_1^0)$ when going from SPS1a' to SPS3 can be understood from the fact that both left sleptons as well as (lightest) neutralino and chargino are approximately a factor of 2 heavier for SPS3 than for SPS1a'. Since $\text{Br}(\mu \rightarrow e + \gamma) \propto 1/m_{\text{SUSY}}^8$ [33] one expects $\text{Br}(\mu \rightarrow e + \gamma)$ to be a factor of more than several hundred lower for SPS3 than for SPS1a'.

The strong dependence of $\text{Br}(\mu \rightarrow e + \gamma)$ on the supersymmetric mass spectrum is also seen in Fig. 8, where we plot $\text{Br}(\mu \rightarrow e + \gamma)$, $\text{Br}(\tilde{\tau}_2 \rightarrow \mu + \chi_1^0)$, and $\text{Br}(\tilde{\tau}_2 \rightarrow e + \chi_1^0)$ versus the mass of $\tilde{\tau}_2$, for light neutrino parameters as before and a fixed value of $M_R = 3 \times 10^{13}$ GeV. Here, the parameters for the point SPS1a have been varied around the slope given in Ref. [56]. Note that $\text{Br}(\mu \rightarrow e + \gamma)$ drops below the current experimental limit for $m_{\tilde{\tau}_2}$ larger than about 250 GeV. In contrast, the $\tilde{\tau}_2$ LFV decay branch-

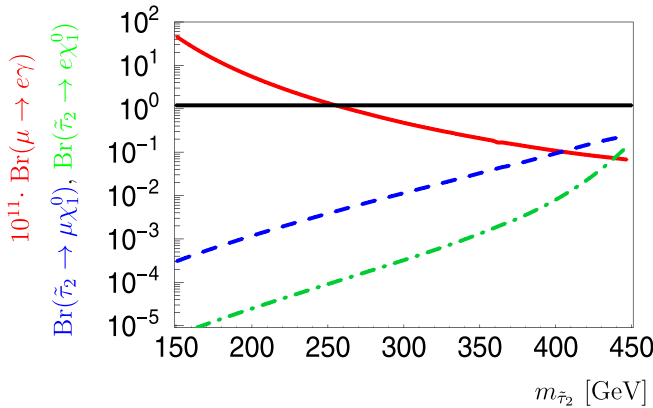


FIG. 8 (color online). Branching ratios as function of scalar tau mass. The full line (red line) is $10^{11} \cdot \text{Br}(\mu \rightarrow e + \gamma)$, the dashed line (blue line) $\text{Br}(\tilde{\tau}_2 \rightarrow \mu + \chi_1^0)$, and the dot-dashed line (green line) is $\text{Br}(\tilde{\tau}_2 \rightarrow e + \chi_1^0)$. The data is calculated for SPS1a with parameters varied along the “slope.” Note that SPS1a is used in this plot instead of SPS1a', since for SPS1a' no slope is given in [57]. Right-handed neutrino mass is fixed to $M_R = 3 \times 10^{13}$ GeV. The black line is the current upper limit on $\text{Br}(\mu \rightarrow e + \gamma)$. While SPS1a with $M_R = 3 \times 10^{13}$ GeV is excluded by $\text{Br}(\mu \rightarrow e + \gamma)$, for slightly heavier slepton masses the low-energy constrained can be evaded, having at the same time sizeable lepton flavor violating slepton decay branching ratios.

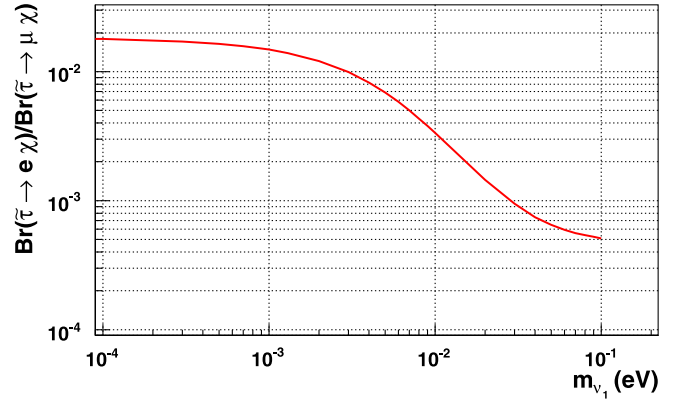


FIG. 9 (color online). Numerically calculated $\text{Br}(\tilde{\tau}_2 \rightarrow e + \chi_1^0)/\text{Br}(\tilde{\tau}_2 \rightarrow \mu + \chi_1^0)$ for the standard point SPS1a' versus lightest neutrino mass for the case of normal hierarchy (compare to Fig. 1).

ing ratios increase for increasing $m_{\tilde{\tau}_2}$. This is due to the fact that left sleptons become more degenerate when m_0 is increased along the slope for SPS1a. The more degenerate sleptons are, the larger the resulting LFV parameters, for given light neutrino parameters. Note, however, that the ratio $\text{Br}(\tilde{\tau}_2 \rightarrow e + \chi_1^0)/\text{Br}(\tilde{\tau}_2 \rightarrow \mu + \chi_1^0)$ remains constant in agreement with the analytical estimate, as long as $\text{Br}(\tilde{\tau}_2 \rightarrow \mu + \chi_1^0)$ is smaller than a few percent. Again this reflects the fact that the small-angle approximation is valid only for small branching ratios in the LFV decays.

We have also checked numerically the reliability of our analytical calculation for the case of $m_1 \neq 0$. An example is shown in Fig. 9. Here we have fixed the mSugra parameters to the standard point SPS1a', the right-handed neutrino mass scale to $M_R = 5 \times 10^{12}$ GeV, the light neutrino mixing angles to the TBM values, Δm_A^2 and Δm_\odot^2 to their b.f.p. values and we have calculated $\text{Br}(\tilde{\tau}_2 \rightarrow e + \chi_1^0)/\text{Br}(\tilde{\tau}_2 \rightarrow \mu + \chi_1^0)$ as a function of the lightest neutrino mass. As shown in Fig. 9 the value of this ratio obtained within a full numerical calculation follows very closely the central value given in Fig. 1, as expected (here we assumed the case of normal hierarchy).

B. Hierarchical right-handed neutrinos

Now we turn to the extreme case of very hierarchical right-handed neutrinos. Again our goal is to check the reliability of the analytical calculation for this case. In all figures presented in this subsection we have taken two of the three right-handed neutrino masses to be constant at $M_R = 10^{10}$ GeV and varied the remaining third right-handed neutrino mass in the ranges given in the figures. In all cases we have fixed the neutrino angles to the TBM values, Δm_A^2 and Δm_\odot^2 to their best-fit values and assumed normal hierarchical neutrinos. The remaining free parameter m_1 is given in each figure.

Figure 10 shows LFV lepton decays as a function of M_1 for $m_1 = 0.001$ eV (left) and for $m_1 = 0.1$ eV (right) for

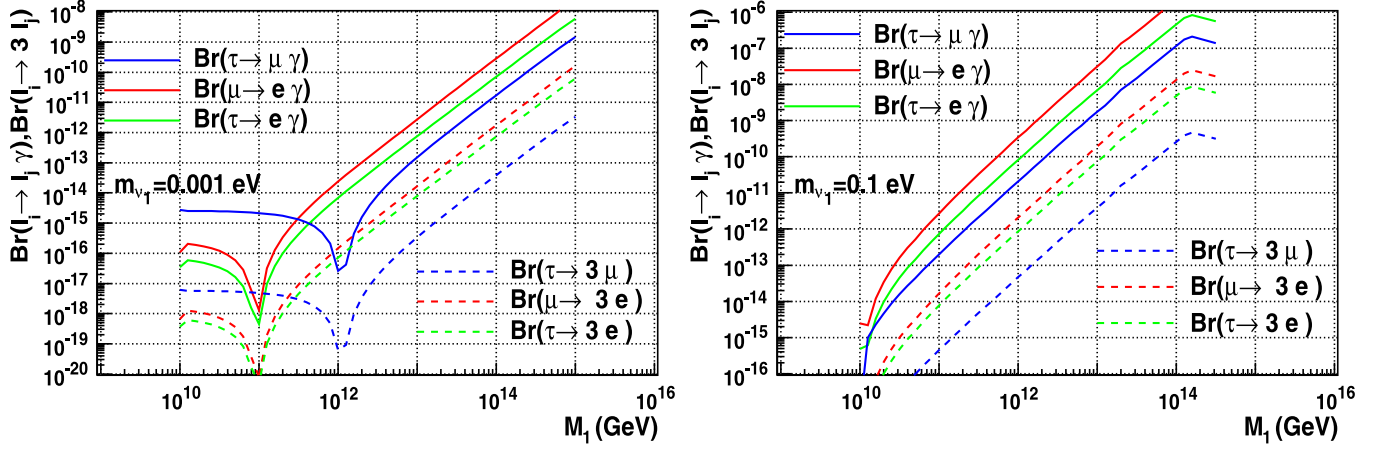


FIG. 10 (color online). Branching ratios for $l_i \rightarrow l_j + \gamma$ and $l_i \rightarrow 3l_j$, as a function of M_1 for constant $M_2 = M_3 = 10^{10}$ GeV and $m_1 = 0.001$ eV (left) and for $m_1 = 0.1$ eV (right). mSugra parameters have been fixed to SPS1a'.

the mSugra parameters fixed at SPS1a'. For $m_1 = 0.001$ eV, the curves are not monotonous functions of M_1 . In fact, in the left figure only for $M_1 \geq 10^{12}$ GeV do the different branching fractions follow the analytical estimates of Eq. (25). This is due to the fact that the different contributions of the M_i to ΔM_{Lij}^2 scale like $m_i M_i \log M_i$, i.e., M_1 becomes dominant in the expressions for the ΔM_{Lij}^2 only if $M_1/M_j \gg m_j/m_1$. This is confirmed by the figure in the right panel, for which $m_1 = 0.1$ eV has been chosen. Here, the contribution from M_1 to the ΔM_{Lij}^2 is indeed the dominant one for $M_1 \geq (\text{few}) \times 10^{10}$ GeV.

Figure 11 shows branching ratios for $\tilde{\tau}_2 \rightarrow e(\mu) + \chi_1^0$ as a function of M_1 for the two mSugra points SPS1a' (left) and SPS3 (right). Again the region excluded by the current upper limit on $\text{Br}(\mu \rightarrow e + \gamma)$ is indicated. Ratios of the LFV slepton decays follow the analytical estimate very well everywhere in the region allowed by the upper limit on $\text{Br}(\mu \rightarrow e + \gamma)$. One observes, as is the case also for

degenerate right-handed neutrinos, that for SPS1a' the absolute values for the LFV branching ratios are too small to be observable, whereas for the mSugra point SPS3 much larger values for LFV scalar tau decays are allowed. Note that $\text{Br}(\tilde{\tau}_2 \rightarrow e + \chi_1^0)$ is larger than $\text{Br}(\tilde{\tau}_2 \rightarrow \mu + \chi_1^0)$ for M_1 dominance, in contrast with the case of degenerate right-handed neutrinos.

Figure 12 shows branching ratios for $l_i \rightarrow l_j + \gamma$ and $l_i \rightarrow 3l_j$ (left) and LFV stau decays (right), for the standard point SPS3 as a function of M_2 . As in Fig. 10, the left panel illustrates that only for $M_2 \geq 10^{12}$ GeV the contribution from M_2 to the LFV mixing angles is dominant. For $M_2 \geq 10^{12}$ GeV the ratios of branching ratios follow the expectation of Eq. (26). LFV scalar tau decays as large as 1% are allowed in this example. Note also that $\text{Br}(\tilde{\tau}_2 \rightarrow e + \chi_1^0) = \text{Br}(\tilde{\tau}_2 \rightarrow \mu + \chi_1^0)$ for M_2 dominance and TBM neutrino angles.

Finally, Fig. 13 shows branching ratios for $l_i \rightarrow l_j + \gamma$ and $l_i \rightarrow 3l_j$ (left) and LFV stau decays (right), for the

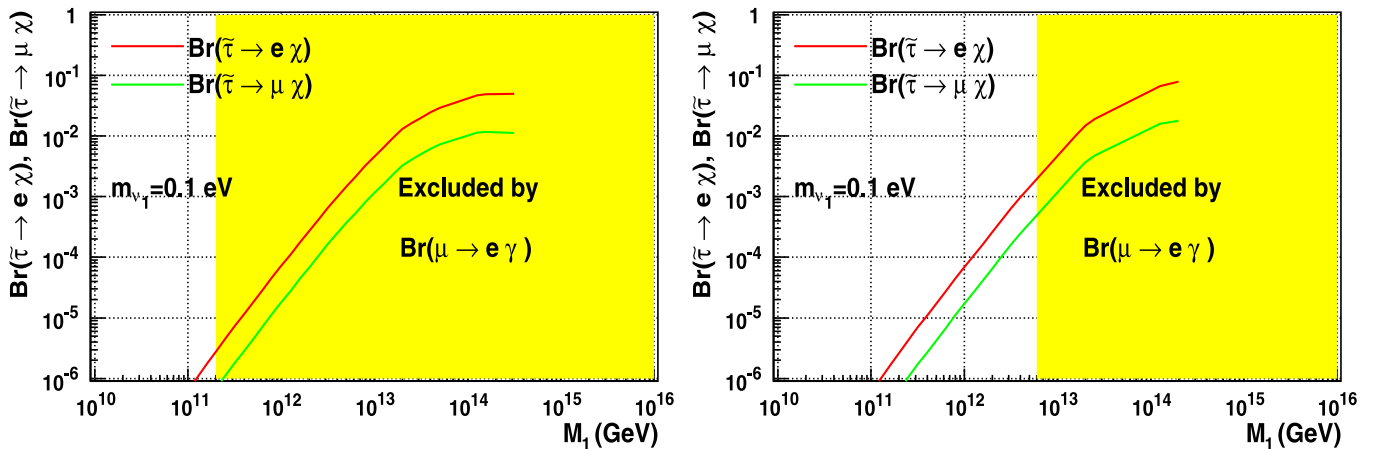


FIG. 11 (color online). Branching ratios for $\tilde{\tau}_2 \rightarrow e(\mu) + \chi_1^0$ as a function of M_1 for constant $M_2 = M_3 = 10^{10}$ GeV for SPS1a' (left) and SPS3 (right).

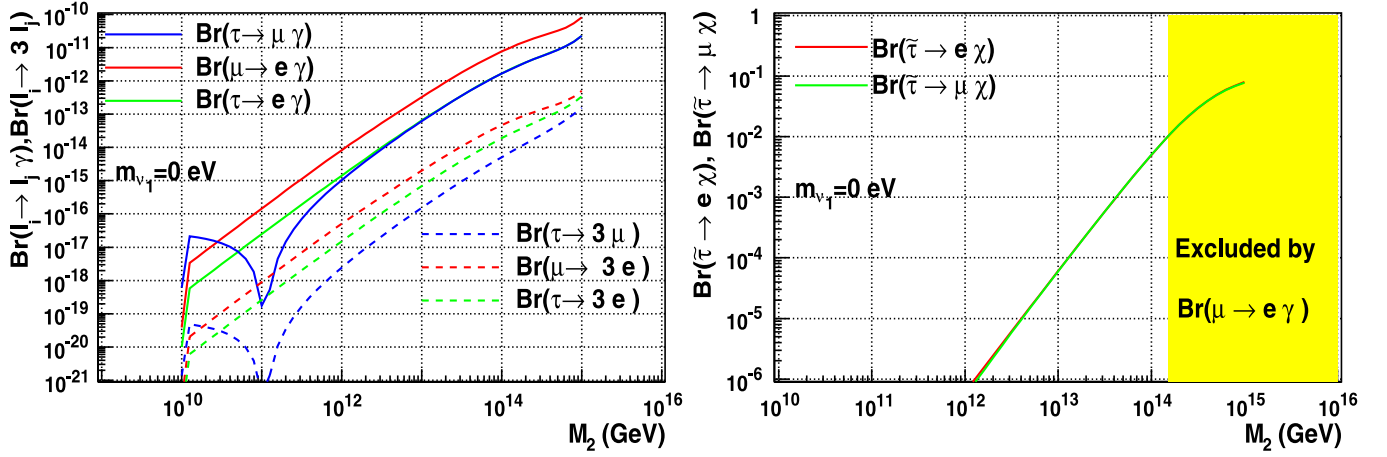


FIG. 12 (color online). Branching ratios for $l_i \rightarrow l_j + \gamma$ and $l_i \rightarrow 3l_j$ (left) and LFV stau decays (right), for the standard point SPS3 as a function of M_2 for constant $M_1 = M_3 = 10^{10}$ GeV.

standard point SPS3 as a function of M_3 fixing $s_{13} \equiv 0$ exactly. This implies that *all* final LFV states involving electrons are tiny, as is expected from Eq. (27). Therefore for $s_{13} \equiv 0$ and M_3 dominance there is no constraint from the upper limit for $\text{Br}(\mu \rightarrow e + \gamma)$. Once s_{13} is nonzero branching ratios for LFV final states involving electrons also become nonzero and proportional to s_{13}^2 .

In summary this section demonstrates that the full numerical calculation confirms the analytical estimates presented above. Absolute values of the LFV branching ratios for lepton decays are sensitive functions of the unknown SUSY spectrum. For light sleptons, usually the constraint from the nonobservation of $\text{Br}(\mu \rightarrow e + \gamma)$ makes the observation of LFV stau decays more likely when M_3 gives the leading contribution to the LFV slepton mixing angles and s_{13} is close to zero. In this case LFV stau branching ratios may exceed 10%, as seen in Fig. 13. LFV stau branching ratios exceeding a percent are also possible for SPS3 for hierarchical right-handed neutrinos and M_1 and

M_2 dominance, as seen in Figs. 11 and 12, but not for the SPS1a' case. Similarly, for the case of degenerate neutrinos, LFV stau branching ratios can exceed a few percent, as seen in Figs. 7, especially for heavier sleptons, say 250–300 GeV, where the $\text{Br}(\mu \rightarrow e + \gamma)$ is smaller than the experimental limit and hence does not place a restriction, as seen in Fig. 8.

Finally we note that we have expressed our results in terms of branching ratios. To get a rough idea on the observability of the signal, one has also to consider cross sections and backgrounds. For the signal itself one would have to work out a detailed set of cuts to suppress background which is clearly beyond the scope of the present work. However, after applying basic cuts used for SUSY signals [62] one can estimate the cross sections for $\tilde{\tau}_2$ production. Using PYTHIA 6.4 [63] we find for the sum of all (Drell-Yan) cross sections 126 fb (25 fb) and 31 fb (3 fb) for $\tilde{\tau}_2$ in cascade decays in the case of SPS1a' (SPS3). Based on Monte Carlo analysis [64,65] it has been shown

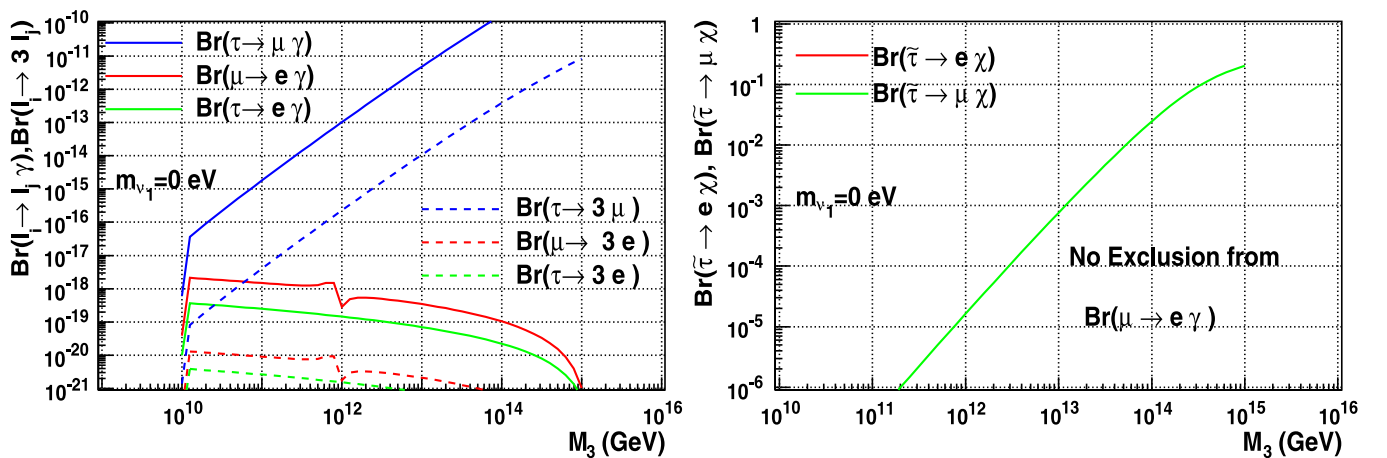


FIG. 13 (color online). Branching ratios for $l_i \rightarrow l_j + \gamma$ and $l_i \rightarrow 3l_j$ (left) and LFV stau decays (right), for the standard point SPS3 as a function of M_3 for constant $M_1 = M_2 = 10^{10}$ GeV.

that lepton flavor violation can be observed in dilepton invariant mass spectra within SUSY cascade decays. There the largest SM background is due to $t\bar{t}$ production. There is also SUSY background due to uncorrelated leptons stemming from different squark and gluino decay chains. The dilepton spectra can provide a distinct signal of lepton flavor violation, namely, the appearance of double peaks [66] due to the fact that not only one but two or more sleptons can contribute to these spectra. In case of Drell-Yan processes the main background will be W production. To show more clearly the observability of such LFV signals a detailed Monte Carlo study would be necessary. This, however, is beyond the scope of the present paper.

We have shown results only for two standard mSugra points. However, as mentioned above, we have checked with a number of other points that *ratios of branching ratios* to a good approximation do not depend on the mSugra parameters. For absolute values of the branching ratios in general a heavier slepton spectrum leads to smaller LFV rates at low-energy and larger LFV branching ratios at the LHC become possible, see also Fig. 8. Heavier sleptons, on the other hand, will lead to lower Drell-Yan production cross section, such that stau production will be dominated by cascade decays, the exact number of events depending on the details of the SUSY spectrum. We plan to do a more detailed, quantitative study of absolute event rates over all of mSugra space in the future.

V. CONCLUSIONS AND OUTLOOK

We have calculated lepton flavor violating processes both in LFV decays of the μ and the τ leptons, as well as branching ratios for LFV stau decays in the supersymmetric version of the minimal type I seesaw mechanism with mSugra boundary conditions. We have limited ourselves to the study of a few standard mSugra points, ratios of LFV branching ratios are independent of this choice and therefore an interesting instrument to study the unknown seesaw parameters.

We have shown that the LFV branching ratios for lepton decays are sensitive functions of the unknown SUSY spectrum. For light sleptons, the nonobservation of $\text{Br}(\mu \rightarrow e + \gamma)$ places an important constraint on the observability of LFV stau decays. The most favorable case is when right-

handed neutrinos are hierarchical, with M_3 giving the leading contribution to the LFV slepton mixing angles and s_{13} close to zero. In this case LFV stau branching ratios may exceed 10% or so, see Fig. 13. LFV stau branching ratios exceeding the percent level may also occur for hierarchical right-handed neutrinos with M_1 or M_2 dominance for the SPS3 reference point, but not for the SPS1a' case, see Figs. 11 and 12. Similarly, for the case of degenerate neutrinos, LFV stau branching ratios can exceed a few percent, as seen in Figs. 7, especially for sleptons heavier than 250 GeV or so, as seen in Fig. 8.

Notice that the above results rely crucially on an important simplifying assumption about the right-handed neutrino spectrum. For example, for degenerate right-handed neutrinos they require that R be real, while for hierarchical right-handed neutrinos they hold when $R = 1$. This simplification allows one to calculate LFV decays of leptons and of the scalar tau as a function of low-energy neutrino parameters. However the use of this assumption should be critically scrutinized. We plan to come back to this issue in a future publication. Once an improved experimental determination of m_1 and s_{13} becomes available from future double beta decay and neutrino oscillation studies at reactor and accelerators, one could start “learning” about the right-handed neutrino sector, once the correct SUSY breaking scheme has been identified and provided that the SUSY breaking scale is above the lepton number breaking scale.

ACKNOWLEDGMENTS

Work supported by Spanish Grants No. FPA2005-01269 and Accion Integrada HA-2007-0090 (MEC) and by the European Commission network MRTN-CT-2004-503369 and ILIAS/N6 RII3-CT-2004-506222. The work of A. V. M. is supported by *Fundação para a Ciência e a Tecnologia* under Grant No. SFRH/BPD/30450/2006. W.P. is partially supported by the German Ministry of Education and Research (BMBF) under Contract No. 05HT6WWA, by the DAAD, Project No. D/07/13468 and by the 'Fonds zur Förderung der wissenschaftlichen Forschung' (FWF) of Austria, Project No. P18959-N16.

-
- [1] Y. Fukuda *et al.* (Super-Kamiokande Collaboration), Phys. Rev. Lett. **81**, 1562 (1998); Q.R. Ahmad *et al.* (SNO Collaboration), Phys. Rev. Lett. **89**, 011301 (2002); K. Eguchi *et al.* (KamLAND Collaboration), Phys. Rev. Lett. **90**, 021802 (2003).
 [2] MINOS Collaboration, arXiv:0708.1495.

- [3] S. Abe *et al.* (KamLAND Collaboration), arXiv: 0801.4589.
 [4] M. Maltoni, T. Schwetz, M. A. Tortola, and J. W. F. Valle, New J. Phys. **6**, 122 (2004), arXiv version 6 in hep-ph/0405172 provides updated neutrino oscillation results and references to previous works.

- [5] For a recent review on future double beta experiments, see for example: F. T. Avignone, S. R. Elliott, and J. Engel, *Rev. Mod. Phys.* **80**, 481 (2008); A brief summary of the phenomenology of double beta decay can be found in: M. Hirsch, arXiv:hep-ph/0609146.
- [6] F. Ardellier *et al.* (Double Chooz Collaboration), arXiv: hep-ex/0606025.
- [7] X. Guo *et al.* (Daya Bay Collaboration), arXiv:hep-ex/0701029.
- [8] J. Schechter and J. W. F. Valle, *Phys. Rev. D* **22**, 2227 (1980).
- [9] S. Weinberg, *Phys. Rev. Lett.* **43**, 1566 (1979); *Phys. Rev. D* **22**, 1694 (1980).
- [10] G. Altarelli and F. Feruglio, *New J. Phys.* **6**, 106 (2004); J. W. F. Valle, *J. Phys. Conf. Ser.* **53**, 473 (2006), review based on lectures at the Corfu Summer Institute on Elementary Particle Physics in September 2005.
- [11] A. Zee, *Phys. Lett.* **93B**, 389 (1980).
- [12] K. S. Babu, *Phys. Lett. B* **203**, 132 (1988).
- [13] L. J. Hall and M. Suzuki, *Nucl. Phys.* **B231**, 419 (1984).
- [14] G. G. Ross and J. W. F. Valle, *Phys. Lett.* **151B**, 375 (1985); J. R. Ellis *et al.*, *Phys. Lett.* **150B**, 142 (1985).
- [15] J. C. Romao and J. W. F. Valle, *Nucl. Phys.* **B381**, 87 (1992).
- [16] M. Hirsch *et al.*, *Phys. Rev. D* **62**, 113008 (2000); **65**, 119901(E) (2002).
- [17] M. A. Diaz *et al.*, *Phys. Rev. D* **68**, 013009 (2003).
- [18] M. Hirsch, H. V. Klapdor-Kleingrothaus, and S. G. Kovalenko, *Phys. Lett. B* **378**, 17 (1996).
- [19] R. N. Mohapatra and J. W. F. Valle, *Phys. Rev. D* **34**, 1642 (1986).
- [20] D. Aristizabal Sierra and D. Restrepo, *J. High Energy Phys.* **08** (2006) 036.
- [21] D. Aristizabal Sierra and M. Hirsch, *J. High Energy Phys.* **12** (2006) 052.
- [22] M. Nebot, J. F. Oliver, D. Palao, and A. Santamaria, *Phys. Rev. D* **77**, 093013 (2008).
- [23] D. Aristizabal Sierra, M. Hirsch, and S. G. Kovalenko, *Phys. Rev. D* **77**, 055011 (2008).
- [24] M. Hirsch, W. Porod, J. C. Romao, and J. W. F. Valle, *Phys. Rev. D* **66**, 095006 (2002).
- [25] P. Minkowski, *Phys. Lett.* **67B**, 421 (1977).
- [26] M. Gell-Mann, P. Ramond, and R. Slansky, in *Supergravity*, edited by P. van Nieuwenhuizen and D. Freedman (North Holland, Amsterdam, 1979).
- [27] T. Yanagida, in *KEK Lectures*, edited by O. Sawada and A. Sugamoto (KEK, Tsukuba, Japan, 1979); M. Gell-Mann, P. Ramond, and R. Slansky, in *Supergravity*, edited by P. van Nieuwenhuizen and D. Freedman (North Holland, Amsterdam, 1979).
- [28] R. N. Mohapatra and G. Senjanovic, *Phys. Rev. Lett.* **44**, 91 (1980).
- [29] J. Schechter and J. W. F. Valle, *Phys. Rev. D* **25**, 774 (1982).
- [30] L. J. Hall, V. A. Kostelecky, and S. Raby, *Nucl. Phys.* **B267**, 415 (1986).
- [31] F. Borzumati and A. Masiero, *Phys. Rev. Lett.* **57**, 961 (1986).
- [32] J. Hisano, T. Moroi, K. Tobe, M. Yamaguchi, and T. Yanagida, *Phys. Lett. B* **357**, 579 (1995).
- [33] J. Hisano, T. Moroi, K. Tobe, and M. Yamaguchi, *Phys. Rev. D* **53**, 2442 (1996).
- [34] F. Deppisch, H. Paes, A. Redelbach, R. Ruckl, and Y. Shimizu, *Eur. Phys. J. C* **28**, 365 (2003).
- [35] E. Arganda and M. J. Herrero, *Phys. Rev. D* **73**, 055003 (2006).
- [36] S. Antusch, E. Arganda, M. J. Herrero, and A. M. Teixeira, *J. High Energy Phys.* **11** (2006) 090.
- [37] F. Deppisch and J. W. F. Valle, *Phys. Rev. D* **72**, 036001 (2005).
- [38] E. Arganda, M. J. Herrero, and A. M. Teixeira, *J. High Energy Phys.* **10** (2007) 104.
- [39] F. Deppisch, T. S. Kosmas, and J. W. F. Valle, *Nucl. Phys.* **B752**, 80 (2006).
- [40] J. Hisano, M. M. Nojiri, Y. Shimizu, and M. Tanaka, *Phys. Rev. D* **60**, 055008 (1999).
- [41] G. A. Blair, W. Porod, and P. M. Zerwas, *Eur. Phys. J. C* **27**, 263 (2003).
- [42] A. Freitas, W. Porod, and P. M. Zerwas, *Phys. Rev. D* **72**, 115002 (2005).
- [43] M. R. Buckley and H. Murayama, *Phys. Rev. Lett.* **97**, 231801 (2006).
- [44] F. Deppisch, A. Freitas, W. Porod, and P. M. Zerwas, *Phys. Rev. D* **77**, 075009 (2008).
- [45] J. R. Ellis, J. Hisano, M. Raidal, and Y. Shimizu, *Phys. Rev. D* **66**, 115013 (2002).
- [46] J. Bernabeu *et al.*, *Phys. Lett. B* **187**, 303 (1987).
- [47] J. A. Casas and A. Ibarra, *Nucl. Phys.* **B618**, 171 (2001).
- [48] H. E. Haber and G. L. Kane, *Phys. Rep.* **117**, 75 (1985).
- [49] S. P. Martin, arXiv:hep-ph/9709356.
- [50] S. Antusch and M. Ratz, *J. High Energy Phys.* **07** (2002) 059.
- [51] H. Nunokawa, S. J. Parke, and J. W. F. Valle, *Prog. Part. Nucl. Phys.* **60**, 338 (2008).
- [52] S. Davidson, arXiv:hep-ph/0409339.
- [53] M. Hirsch, S. Morisi, and J. W. F. Valle, arXiv:0804.1521.
- [54] P. F. Harrison, D. H. Perkins, and W. G. Scott, *Phys. Lett. B* **530**, 167 (2002).
- [55] W. Porod, *Comput. Phys. Commun.* **153**, 275 (2003).
- [56] B. C. Allanach *et al.*, *Eur. Phys. J. C* **25**, 113 (2002).
- [57] J. A. Aguilar-Saavedra *et al.*, *Eur. Phys. J. C* **46**, 43 (2006).
- [58] S. Antusch, J. Kersten, M. Lindner, M. Ratz, and M. A. Schmidt, *J. High Energy Phys.* **03** (2005) 024.
- [59] F. James and M. Roos, *Comput. Phys. Commun.* **10**, 343 (1975).
- [60] J. Hisano and D. Nomura, *Phys. Rev. D* **59**, 116005 (1999).
- [61] W. M. Yao *et al.* (Particle Data Group), *J. Phys. G* **33**, 1 (2006).
- [62] G. L. Bayatian *et al.*, CMS Collaboration, CMS Physics Technical Design Report, vol. 1. CERN, Geneva, 2006, CMS Note CERN/LHCC 2006-001.
- [63] T. Sjostrand, S. Mrenna, and P. Skands, *J. High Energy Phys.* **05** (2006) 026.
- [64] I. Hinchliffe and F. E. Paige, *Phys. Rev. D* **63**, 115006 (2001).
- [65] J. Hisano, R. Kitano, and M. M. Nojiri, *Phys. Rev. D* **65**, 116002 (2002).
- [66] A. Bartl *et al.*, *Eur. Phys. J. C* **46**, 783 (2006).